Spring 2015

Effect of impeller submergence on power dissipation and solids suspension in mixing systems equipped with pitch-blade turbines

Yufeng Song
New Jersey Institute of Technology

ABSTRACT

EFFECT OF IMPELLER SUBMERGENCE ON POWER DISSIPATION AND SOLIDS SUSPENSION IN MIXING SYSTEMS EQUIPPED WITH PITCH-BLADE TURBINES

By

Yufeng Song

Mixing and dispersion of solids in a liquid is a process frequently encountered in the pharmaceutical industry and often conducted in cylindrical baffled tanks stirred by mechanical impellers. In operations where the liquid level is decreased (as often which emptying the tank) the process must be stopped when the solids are no longer suspended. In this work, the minimum agitation to suspend solids (N_{js}) when the liquid level was lowered, and the impeller submergence S_b changed as a result were determined for the case of a six-blade, pitch-blade turbine (6-PBT) impeller. The power consumed by the impeller was also measured. It was found that when a critical impeller submerge level was reached it was impossible to suspend the solids and the impeller power decreased significantly, although the impeller was still full submerged. The results are important to ensure that mixing systems are operated properly.

EFFECT OF IMPELLER SUBMERGENCE ON POWER DISSIPATION AND SOLIDS SUSPENSION IN MIXING SYSTEMS EQUIPPED WITH PITCH-BLADE TURBINES

by
Yufeng Song

A Thesis
Submitted to the Faculty of
New Jersey Institute of Technology
in Partial Fulfillment of the Requirements for the Degree of
Master of Science in Pharmaceutical Engineering

Otto H. York Department of Chemical, Biological and Pharmaceutical Engineering

May 2015

Blank Page

APPROVAL PAGE

EFFECT OF IMPELLER SUBMERGENCE ON POWER DISSIPATION AND SOLIDS SUSPENSION IN MIXING SYSTEMS EQUIPPED WITH PITCH-BLADE TURBINES

Yufeng Song

Dr. Piero M. Armenante, Thesis Advisor Date
Distinguished Professor of Chemical, Biological and Pharmaceutical Engineering, NJIT

Dr. Kamalesh K Sirkar, Committee Member Date
Distinguished Professor of Chemical, Biological and Pharmaceutical Engineering, NJIT

Dr. Xianqin Wang, Committee Member Date
Associate Professor of Chemical, Biological and Pharmaceutical Engineering, NJIT

BIOGRAPHICAL SKETCH

Author: Yufeng Song

Degree: Master of Science

Date: May 2015

Undergraduate and Graduate Education:

Master of Science in Pharmaceutical Engineering,
New Jersey Institute of Technology, Newark, NJ, 2015

Bachelor of Science in Pharmaceutical Science,
Shandong University, Jinan, P. R. China, 2012

Major: Pharmaceutical Engineering

To My Friends

ACKNOWLEDGMENT

I owe my gratitude to all those people who have made this thesis possible and because of whom my graduate experience has been one that I will cherish forever.

My deepest gratitude is to my advisor, Dr. Piero Armenante. I have been amazingly fortunate to have an advisor who gave me the freedom to explore on my own, and at the same time the guidance to recover when my steps faltered. Dr. Armenante taught me how to question thoughts and express ideas. His patience and support helped me overcome many crisis situations and finish this thesis.

I would like to acknowledge Dr. Kamalesh Sirkar and Dr. Xianqin Wang for their patience in reviewing the thesis, for their recommendations and everything

TABLE OF CONTENTS

LIST OF TABLES

LIST OF FIGURES

NOMENCLATURE

D	Impeller diameter (m)
T	Tank diameter (m)
H	Liquid height (m)
C_b	Bottom clearance (distance from bottom of the impeller blades to the tank bottom) (m)
C_b/T	Impeller off-bottom clearance ratio(-)
H/T	Fill ratio (-)
v	Kinematic viscosity (m^2/s)
N	Agitation speed (rpm)
N_{js}	Minimum agitation speed for solid suspension (rpm)
P	Instantaneous power dissipated by the impeller (watt)
P_{js}	The power dissipated by the impeller for complete off-bottom solid suspension at the N_{js} (watt)
Po	Impeller Power Number (-)
ρ	Liquid density (kg/m^3)
Re	Reynolds Number
S_b	Impeller submergence (distance from bottom of the impeller blades to the air-liquid interface) (m)
S_b/D	Impeller submergence ratio (-)
τ	Torque (Nm)
δ_B	Gap between baffles and tank (m)

CHAPTER 1

INTRODUCTION

1.1 Background

The term "mixing" refers to all those operations that tend to reduce non-uniformity in one or more of the properties of a material in bulk (e.g., concentration, temperature).Mixing of a liquid with other media (fine solids, gas, immiscible liquid) is an extremely common operation encountered in countless applications in the pharmaceutical industry. In the pharmaceutical industry many mixing, reaction, and mass transfer operations are conducted in stirred tanks and reactors.

Stirred vessels are commonly used in industry to achieve the desired process objectives. Over 50% of chemical, pharmaceutical, and food production takes place in batch stirred-tank/reactors. Quality of mixing is important: poor mixing leads to off-spec products; both under-mixing and over-mixing must be considered.

In the industrial practice, mixing of solid in liquid is often conducted in cylindrical baffled tanks stirred by mechanical agitators. The role of baffles in a mechanically agitated vessel is to promote the stability of power drawn by the impeller and to prevent swirling and vortexing of liquid, thus, greatly improving the mixing of liquid. (Myers et al., 2002).

The performance of any mixing operation in a stirred tank/reactor is intimately related to the hydrodynamics of the liquid or multiphase system in the mixing vessel/reactor. Most tanks and reactors in industry are operated with a liquid height-to-tank diameter ratio equal to or larger than one ($H/T \geq 1$). The hydrodynamics for such systems has been extensively studied. H/T=1 is the H/T ratio most commonly studied for stirred tanks. However, there are many instances where H/T <1. For examples, emptying/charging batch stirred reactors and vessels, or adding reactants and solvents. The type of flow pattern observed in a stirred tank can also be affected by the impeller submergence (S_b) and the impeller submergence-to-impeller diameter ratio (S_b/D ratio), especially if the submergence is low. At low impeller submergence induced surface air entrainment may also occur, possibly resulting in impeller flooding.

Previous work was conducted by Dr. Piero Armenante's group on the effect of S_b/D on flow pattern and power dissipation for the case of a radial impeller (Disk Turbine) (Motamedvaziri, S. and Armenante, P. M., 2012). The graduate student Anqi Zhou (2013) used Zwietering's method to measure N_{js} by visually inspecting. Previous work by Armenante et al. and Armenante and Uehara Nagamine (1997,1998) determined the minimum agitation speed and power dissipation required to completely suspend solid particles in tanks provided with six-blade (45°) pitched-blade turbines impellers having small clearances off the tank bottom, and studied the effects of the impeller diameter, tank diameter, particle diameter, and physical variables. Modified correlations based on the Zwietering equation (Zwietering, 1958) were obtained to account for the effect of impeller clearance and impeller diameter-to-tank diameter ratio on N_{js}.

Geometric and operating variables have a strong impact on different mixing phenomena and mixing parameters, which have a significant effect on the process carried out in the mixing system. Chapple et al. (2002) stated that the power number is independent of blade thickness, but dependent on the impeller to tank diameter ratio (D/T). Chapple et al. (2002) also stated that the different position of the impeller in the tank can have a significant impact on the power number. Power number, Po, is one of the most important variables in the description of mixing phenomena which quantifies the power dissipated by the impeller. The power dissipated by the agitation system is fundamental to any mixing process since energy is needed to homogenize the vessel content, disperse immiscible phases, suspend solids, increase mass transfer, and in general, produce the desired mixing effect. When the impeller submergence is reduced as a result of lowering the liquid level, the mixing performance changes depending on the geometric variables of the system (such as impeller clearance, liquid height, or liquid head above the impeller).

1.2 Objectives of This Work

The objective of this work is to study primarily the effect of S_b/D ratio, but also the effect of other geometric ratios (C_b/T, D/T), on the impeller Power Number and the minimum agitation speed for solid suspension, N_{js}, for six-blade, 45° pitch-blade turbine impellers in flat-bottomed baffled tanks and to determine the critical impeller submergence ratio (S_b/D) for adequate mixing can still be achieved. This was achieved using combinations of different impellers and tank sizes.

CHAPTER 2

EXPERIMENTAL APPARATUS, MATERIALS AND METHODS

2.1 Agitation System

The experimental apparatus, shown in Figure 2.1, consisted of a baffled cylindrical mixing tank with a flat bottom (with right-angle corner or with rounded corner; Figure 2.2), having an internal diameter, *T*. The tank was proved with four baffles having a width of B (*B*=*T/10*). The system is stirred by a single six-blade, 45° pitch-blade turbine (6-PBT; Figure 2.3) impeller having a diameter *D*. Tanks and impellers of different sizes were used here. Their detailed dimensions are shown in Table 2.1 and Table 2.2, respectively.

The selected impeller was mounted to a central located shaft (shaft diameter 12.52 mm) inside the tank, and was rotated by a 0.25 HP motor (Chemglass, Model CG-2033-11) controlled by an external controller (Chemglass, Model CG-2033-31). The motor was equipped with a controller to adjust the agitation speed in the range 0-500 RPM. A traversing system supporting the tank was used to change the vertical position of the tank. A data acquisition system was used to measure the agitation speed, the torque (Γ) applied to the impeller, and the power dissipated by the impeller. The torque applied to the impeller by the motor was experimentally measured using a strain gage-based rotary torque transducer (Model, T6-5-Dual Range, Interface, Inc., Scottsdale, AZ) mounted between the motor and the impeller. The transducer was connected to the Interface series 9850 Multi-Channel Load Cell Indicator. The transducer could measure the torque in two different ranges, i.e., 0-0.5 Nm and 0-5 Nm. The same instrument could also measure the agitation speed via a tachometer. Then the power dissipated by the impeller was calculated from:

$$P = 2\pi N \Gamma \quad \text{(Equation 2.1)}$$

The indicator utilized the M700 software to interface with a computer, which was used for data acquisition and processing.

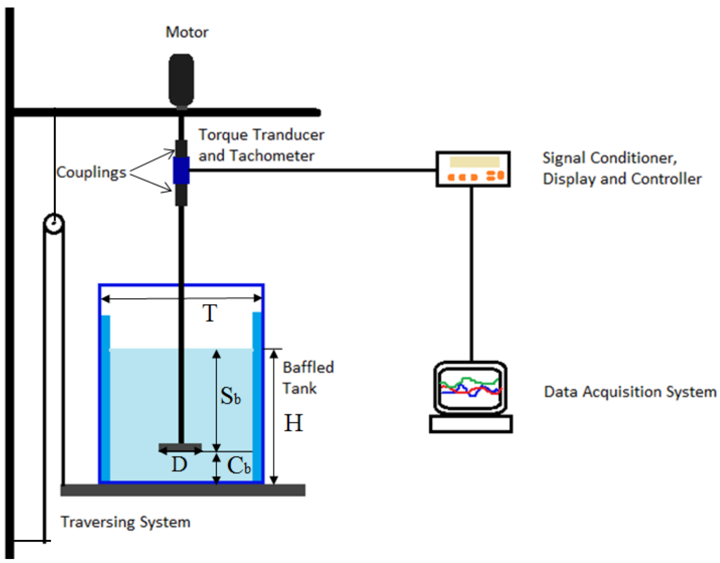

Figure 2.1 Schematic Diagram of the Experimental Apparatus

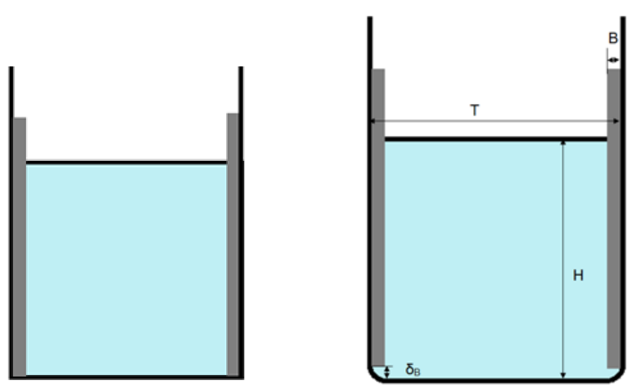

(a) **(b)**

Figure 2.2 Schematic Diagram of the Baffled Flat-Bottom Tanks Used in this Work: (a) Tank #1 and Tank #2 (right-angle corner); (b) Tank #3 (round corner).

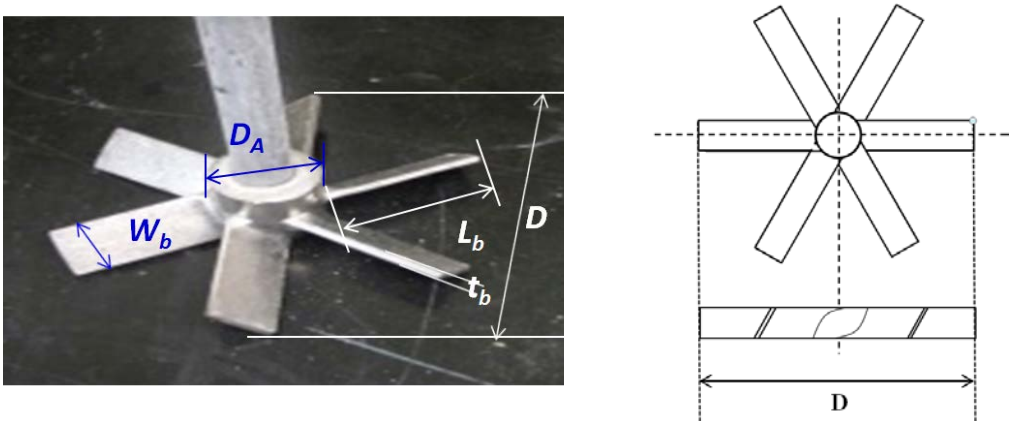

Figure 2.3 Schematic Diagram of Six-blade, 45^0 Pitch-blade turbine (6-PBT) Impellers

Table 2.1 Dimensions of the Baffled Flat-Bottom Tanks Used in this Work

Tank No.	Diameter (T) m	Height (L) m	Baffle Width (W_f) m	Baffle Thickness (t_f) m	Bottom Corner Shape
1	0.189	0.232	0.0189	0.0062	Right Angle
2	0.246	0.331	0.0246	0.0063	Right Angle
3	0.288	0.443	0.0288	0.0095	Round

Table 2.2 Dimensions of the 45^0 6-Blade Disk Turbine (6-PBT) Impellers Used in this Work

Impeller No.	Diameter (D) cm	Axial Diameter cm	Blade width (W_b) cm	Blade Length (L_b) cm	Blade Thickness (t_b) cm
1	6.42	2.51	1.27	1.96	0.18
2	7.54	2.19	1.22	2.61	0.16
3	10.14	2.51	1.73	3.74	0.25

2.2 Materials

Tap water at room temperature was used as the liquid in all experiment (ρ_L= 977 kg/m^3). The liquid height was equal to the tank diameter in all cases. Glass beads having average diameters of 150 µm and 200 µm were used as the dispersed phase (ρ_S= 2650 kg/m^3). Prior to their use, the prescreened glass beads were sieved. Four US standard screens of mesh size 40, 60, 80 and 100 were selected. 30 g of glass beads were processed at a time, by placing them in the top screen with the smallest mesh size, and shaking them for five minutes. The particles retained on the size 100 mesh screen (with an average diameter size of 150 µm) and size 80 mesh screen (with an average diameter size of 200 µm) were collected separately and used in the experiments. In all experiments involving solids, the solid fraction used was 0.5% of the liquid mass (g/g).

2.3 Experimental Determination of the Power Number, Impeller Reynolds Number, and Minimum Agitation Speed

The experimental power dissipation was measured for different combinations of liquid level, impeller size, baffle tank size, impeller clearance and agitation speed. In all experiments, the system was allowed to stabilize for two minutes before colleting power data in at least 20 seconds time intervals. Equation 2.2 and 2.3 were used to obtain the experimental power number, *Po*, and impeller Reynold Number, *Re* seperately.

$$Po = \frac{P}{\rho N^3 D^5} \qquad \text{(Equation 2.2)}$$

$$Re \equiv \frac{\rho N D^2}{\mu} \equiv \frac{N D^2}{\nu} \qquad \text{(Equation 2.3)}$$

Where ρ is the liquid density, N is the impeller speed (rev/sec), and ν is the kinematic viscosity of the water ($\nu = 10^{-6}$ m^2/s, the testing temperature is about 20 ^{0}C).

In solid-liquid suspension studies, the minimum agitation speed for solid suspension, N_{js}, was measured visually in this work. The visual value of N_{js} was obtained using the Zweitering's criterion (Zwietering, 1958), defined as the agitation speed at which no solids remain at the tank base for more than a second or two. The corresponding power and Power Number for the suspension at N_{js} are denoted here as P_{js} and Po_{js}.

All experiments were repeated in triplicates. The power dissipation at each agitation speed was also recorded.

CHAPTER 3

RESULTS AND DISCUSSION

3.1 Effect of Impeller Submergence Ratio (S_b/D) on Power Number (*Po*) in Different Combination of Impellers and Stirred Baffled Tanks at *C/T*=1/3

In this portion of the work, the power number for the stirred baffled tank was obtained experimentally. The system under investigation here produced a "single loop" recirculation flow.

The impeller Power Number for Impeller #3 in Tank #3 (*D/T*=0.35) was experimentally obtained at different agitation speeds (100 – 480 rpm corresponding to *Re* equal to 1×10^4 – 4.6×10^4) for different submergence ratio. The results are shown in Figure 3.1 (as Po vs. Re) and Figure 3.2 (as Po vs. *N*). From these figures one can see that Reynolds number increases with the rise in the impeller agitation speed. The Power Number is a constant when the Reynolds number is adequately high.

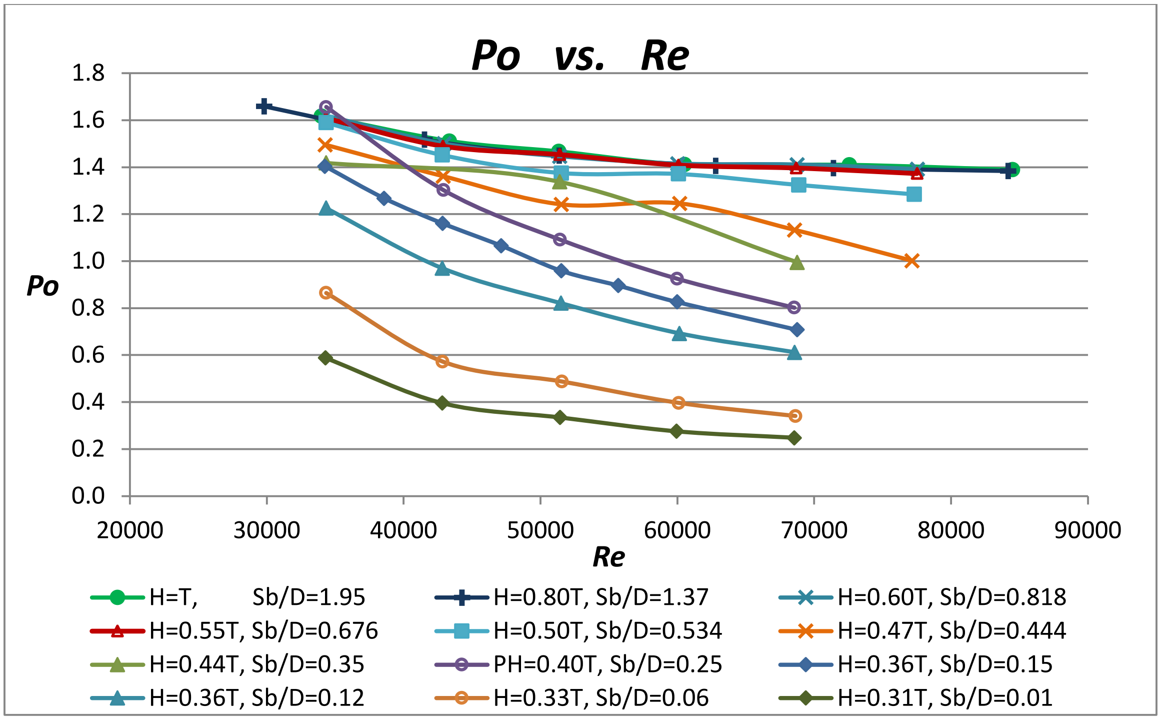

Figure 3.1 The relationship of power number and Reynold number at different submergence ratio (Impeller #3, Tank #3, *D/T*=0.35, *C/T*=1/3).

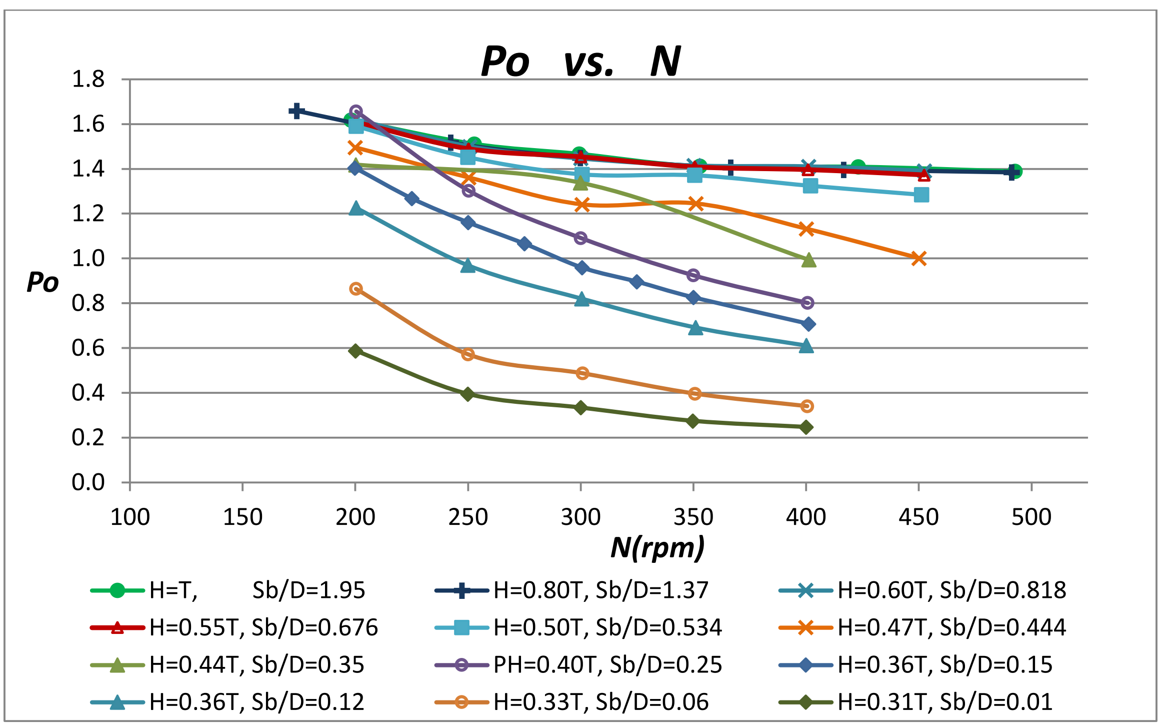

Figure 3.2 The relationship of power number and impeller agitation speed at different submergence ratio (Impeller #3, Tank #3, *D/T*=0.35, *C/T*=1/3).

Figure 3.2 shows that the Power Number is generally constant when the submergence ratio is relativly high (S_b/D>0.6), i.e., when the impeller is well submerged. This can be clearly observed by examining all the power curves for high enough values of the S_b/D which are all superimposed on each other. Figure 3.3 shows a similar trend. Actual data are shown in the Appendix (Table A.1). However, when the impeller submergence ratio decreased below a critical level (S_b/D=0.5 or S_b/T=0.2), the Power Number decreased drastically with S_b/D. In this region, the Power Number was almost directly proportional to the submergence ratio. When the impeller operated above S_b/D>0.6, i.e., just above the critical submergence ratio, no air bubbles were observed. However, when the S_b/D ratio reached a critical value, $(S_b/D)_{cr}$, at about 0.5, bubbles began becoming incorporated in the liquid. As the S_b/D ratio was was further reduced more air was incorporated depending on the agitation speed. In addition, for submergence ratios lower the critical value, the Power Number decreased with increasing agitation speeds, whereas if the submergence ratio was higher than the Power number was largely independent of the agitation speed especially for higher values of N, when, in case, one would expect that aeration was more easily achieved. This can be clearly seen in Figures 3.1 and 3.2, which shows that Po is not a function of Re (or N) when $S_b/D>(S_b/D)_{cr}$, but that Po is a strong function of N when $S_b/D<(S_b/D)_{cr}$, and that Po actually decreases with increasing N values.

This phenomenon appears to be similar to that observed by Motamedvaziri and Armenante (2012) who showed that for a radial impeller there exists a critical value of the the S_b/D ratio below which the flow regime changes. Above this critical value, agitation does not affect Po. However, below this value, the flow regime changes and, if the agitation speed is appropriatedly high, surface aeration starts and the Power number decreases as a result of the air incorporation in the liquid.

A similar phenomenon is likely to occur here. For S_b/D >0.6, the impeller is sufficiently submerged to be "fed" from the top, resulting in the familiar axial flow associated with axial impeller. However, if the submergence is too low, the impeller is no longer able to pump effectively, and surface aeration can occur if the agitation is sufficiently high to displace the fluid surrounding the impeller radially.

Figure 3.3 show this phenomenon even more clearly. At the high agitation speed used in this figure, Po is not affected by the submergence ratio if $S_b/D>(S_b/D)_{cr}$, but it becomes a nearly linear function of S_b/D for $S_b/D<(S_b/D)_{cr}$.

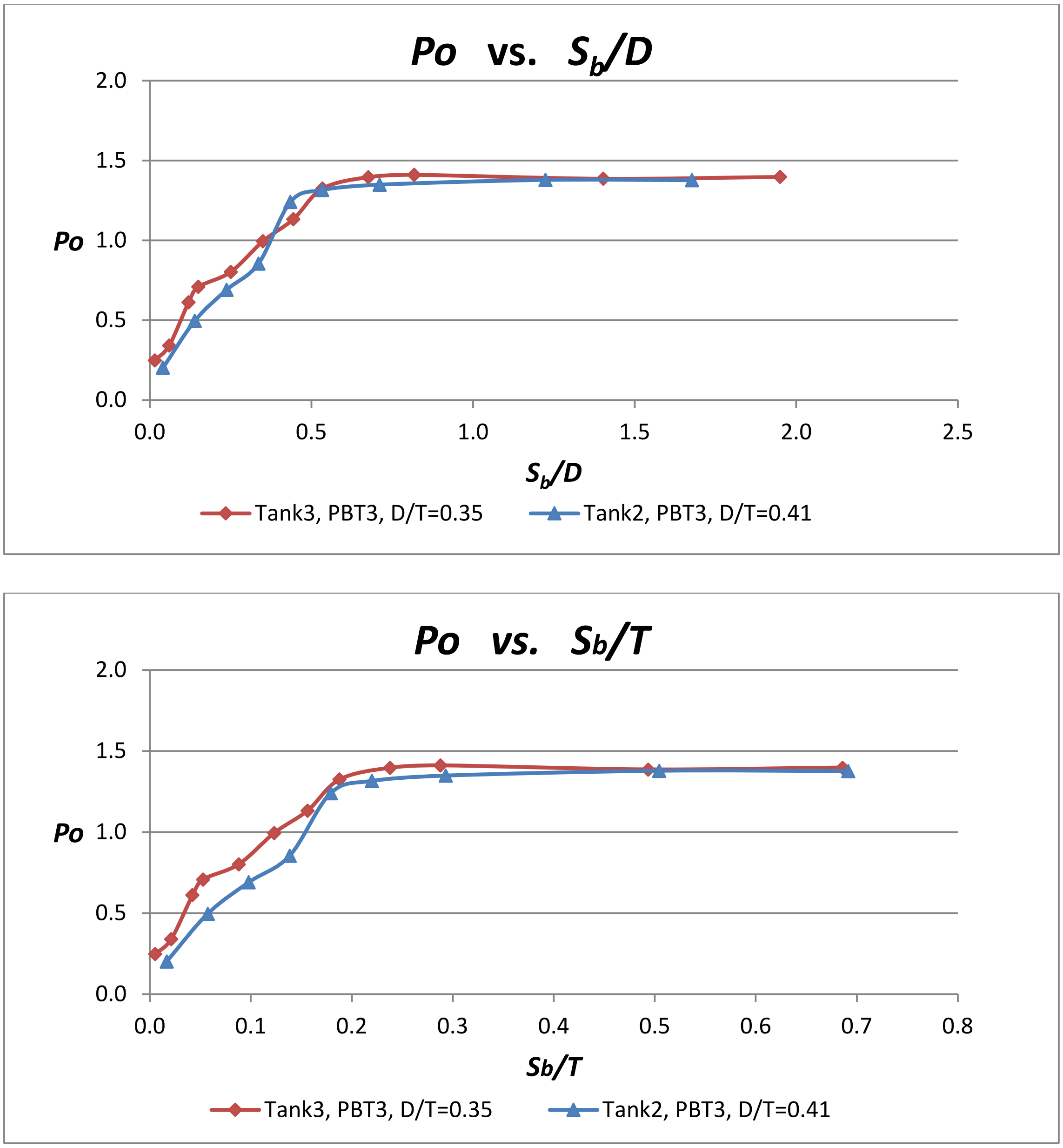

Figure 3.3 Power number, *Po*, for different S_b/D or S_b/T ratios in different combination of impellers and stirred baffled tanks at C/T=1/3 calculated from the experimental data (N=495 rpm).

3.2 Impeller Power Number for *H/T*=1 at Different Combinations of *D/T* and C_b/T Ratios

As it was discussed in the previous section, a typical axial impeller such as a pitched turbine placed in a cylindrical baffled tank filled with a low viscosity liquid typically produces a "single loop" recirculation flow. However, if the impeller off-bottom clearance (C_b) is gradually reduced, a flow pattern transition occurred.

In this section, the effect of impeller off-bottom clearance (C_b), when the *H/T* ratio equals to 1, mixing parameter power number was investigated. Then, for each impeller off-bottom clearance the same phenomena were examined at different impeller submergence S_b/D ratios and fill ratios (*H/T*).

The impeller Power Number as a function of the impeller off-bottom clearance is shown in Figure 3.4. *Po* was nearly constant for impeller off-bottom clearance ratios (C_b/T) from 0.2 to 0.8. In addition, Po was nearly independent of the *D/T* ratio. (data shown in Appendix Table A.2.). These results are similar to those or Armenante et al. (1999).

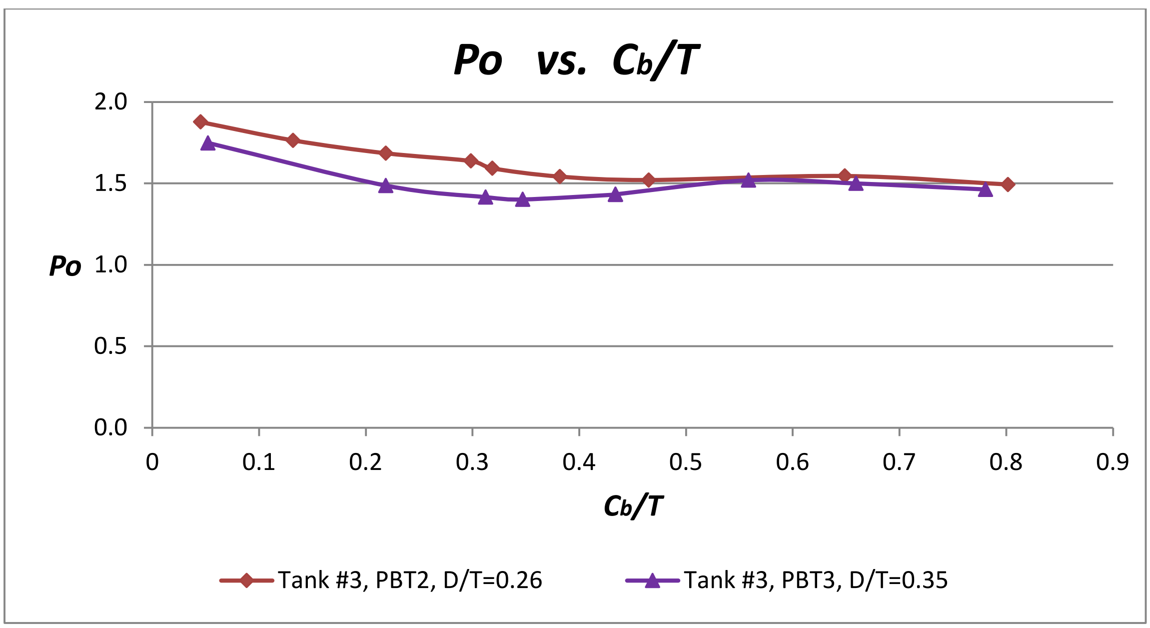

Figure 3.4 Power Number, *Po* for different C_b/T, H/T=1, D/T=0.26 or 0.35, calculated from both experimental data ($N \geq 450$ rpm).

3.3 Solids Suspension in Stirred Baffled Tanks at Different Submergence Ratios and Clearance Ratios

In Section 3.1 and 3.2, the effect of S_b/D on Power Number in stirred baffled tanks with different geometrical variables (C_b/T, D/T) was described. In this section, the effect of C_b/T ratio and S_b/D on the performance of the same mixing systems to achieve complete solid suspension was studied.

Experiments were carried out in the same PBT #2 described in Section 2.1. The liquid phase was water and spherical glass beads (0.5% *wt/wt*; ρ=2500 m^3/kg; diameter 150 μm to 200 μm) were used. The minumum agitation speed required for complete off-bottom particle suspension, N_{js}, was determined visually (as described in Chapter 2.3).

The main objective here was to characterize the effect of impeller submergence ratio (S_b/D) on N_{js} for stirred vessels with different C_b/T and different D/T. N_{js} was obtained for: (1) H/T=1 and different D/T and C_b/T ratios; (2) C_b/T=0.30 and different D/T and S_b/D ratios.

3.3.1 Effect of C_b/T on Minimum Agitation Speed (N_{js}) for Complete Off-Bottom Solid Suspension for H/T=1 and Different D/T

Figure 3.5(a) shows the minimum agitation speed measured at two different impeller D/T ratios (0.31 and 0.40) and same liquid level (H/T=1) as a function of the impeller off-bottom clearance ratio (C_b/T). Figure 3.5(a) also shows that glass beads could be suspended at a lower impeller agitation speed when the D/T ratio increased.

Sharma and Shaikh (2003) illustrated the ralationship of minimum agitation speed for complete off-bottom solids suspension with impeller clearance: at low C/T where the impeller is very close to the tank bottom, the minimum agitation speed and the relevant power remains constant. Figure 3.5(a) and Figure 3.5(b) shows the same outcome. Figure 3.7 shows that the power number at the minimum agitation speed for complete off-bottom solids suspension is inversely proportional to the impeller off-bottom clearance ratios (C_b/T) at low *C/T*. (Data shown in Appendix Table A.3)

Figure 3.5(a) and (b) also show that *D/T* is also affects the minimum agitation speed but that the minimum power for complete off-bottom solid suspension(P_{js}) is independent on *D/T*.

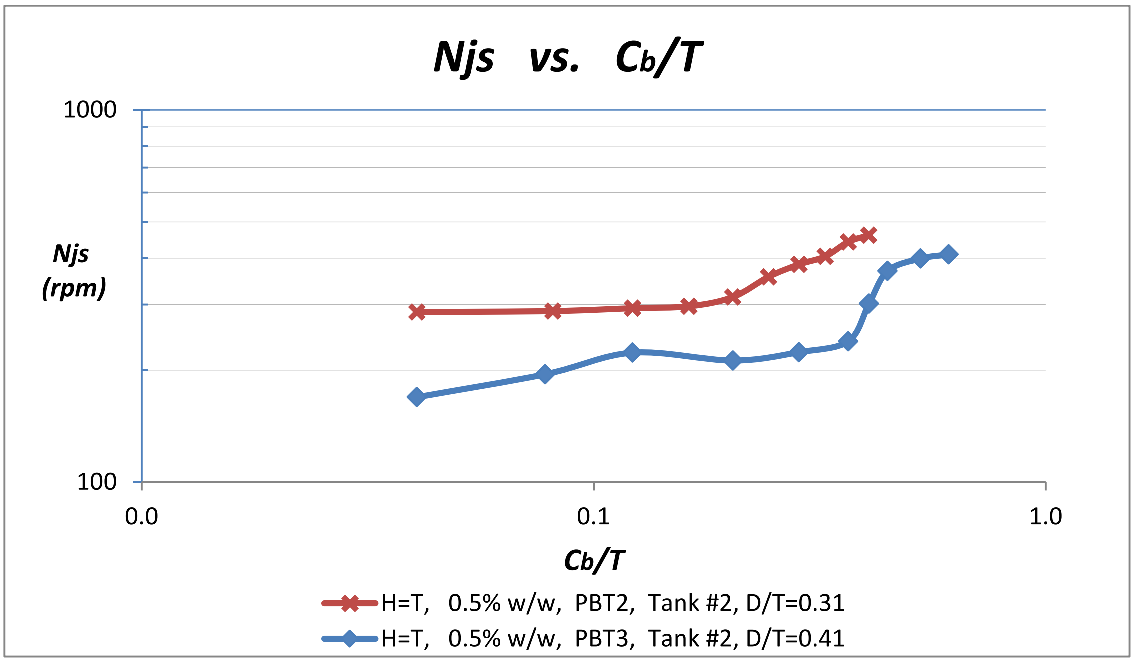

Figure 3.5(a) Minimum agitation speed for complete off-bottom solid suspension (N_{js}) as a function of impeller off-bottom clearance ratios (C_b/T) at different *D/T* ratios.

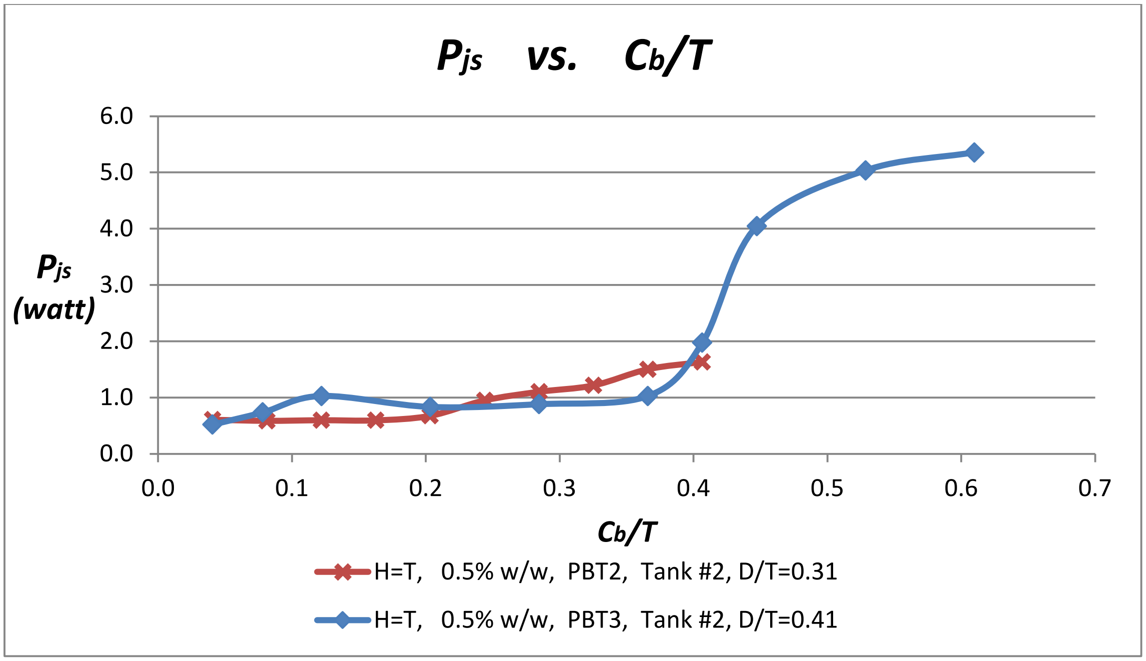

Figure 3.5(b) The minimum power for complete off-bottom solid suspension(P_{js}) as a function of impeller off-bottom clearance ratios (C_b/T) at different D/T ratios.

3.3.2 Effect of S_b/D on Minimum Agitation Speed (N_{js}) for Complete Off-Bottom Solid Suspension for C_b/T=0.30 and Different D/T Ratios

Figure 3.6 shows the minimum agitation speed measured for C_b/T=0.30 or 0.31 at different impeller D/T ratios as a function of the impeller submergence ratio (S_b/D). (Data shown in Appendix Table A.4.) Figure 3.6 also shows that solids could be suspended at a lower agitation speed when D/T ratios increased. A similar phenomenon has been reported by Motamedvaziri and Armenante (2012) in a baffled tank with a disk turbine (DT). For any D/T ratio, there is a critical impeller submergence (S_b/D value), below which solid suspension becomes impossible, irrespective of how high N is, although the impeller is still fully submerged. Solids could be suspended only above this critical S_b/D value

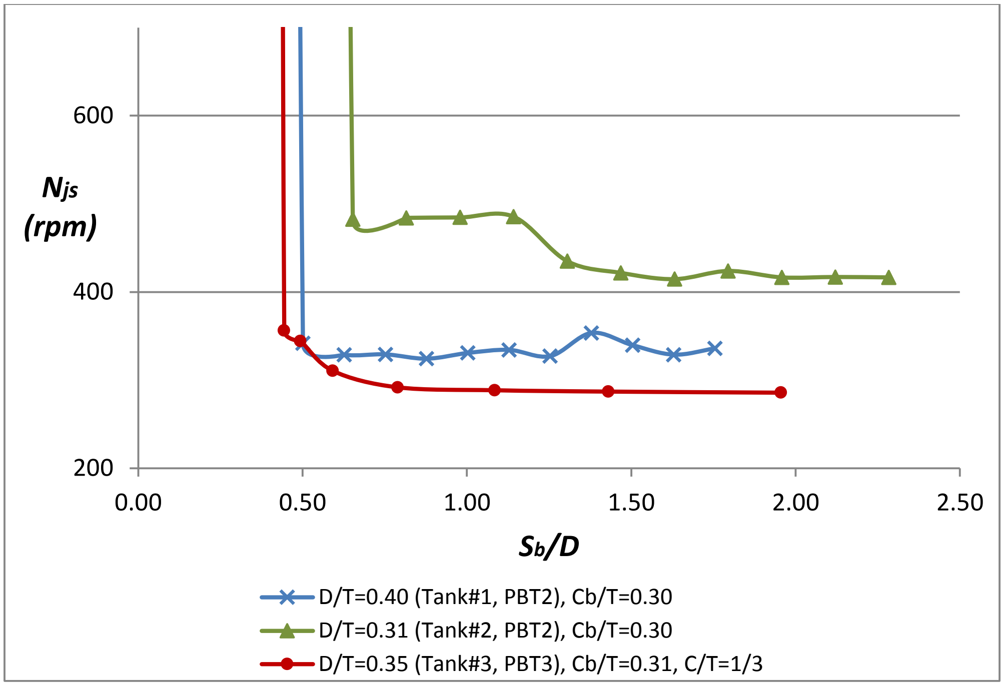

Figure 3.6 Minimum agitation speed for complete off-bottom solid suspension (N_{js}) as a function of impeller submergence ratio for C_b/T=0.30 or 0.31 and different D/T ratios.

Figure 3.6 shows that there is a critical liquid level below which that solids could be suspended for the 6-PBT case as well, i.e., for an axial impeller. For Tank#1 and Tank#2, the minimum level for solid suspension was S_b/D=0.5 and 0.6 for D/T=0.40 and 0.31, respectively.

For Tank #3 with PBT #3, the minimum level for solid suspension was S_b/D=0.44. The range of the critical submergence ratios are exactly the same as those have been get in Section 3.1 as the power number decreased drastically, shown in Figure 3.7.

The results obtained here for the critical agitation speed for solid suspension confirm that a stirred baffled tank operating at low impeller submergence is more likely to experience impeller flooding conditions. The impeller loses its ability to provide sufficient liquid for the entire loop and thus lose complete off-bottom solid suspension.

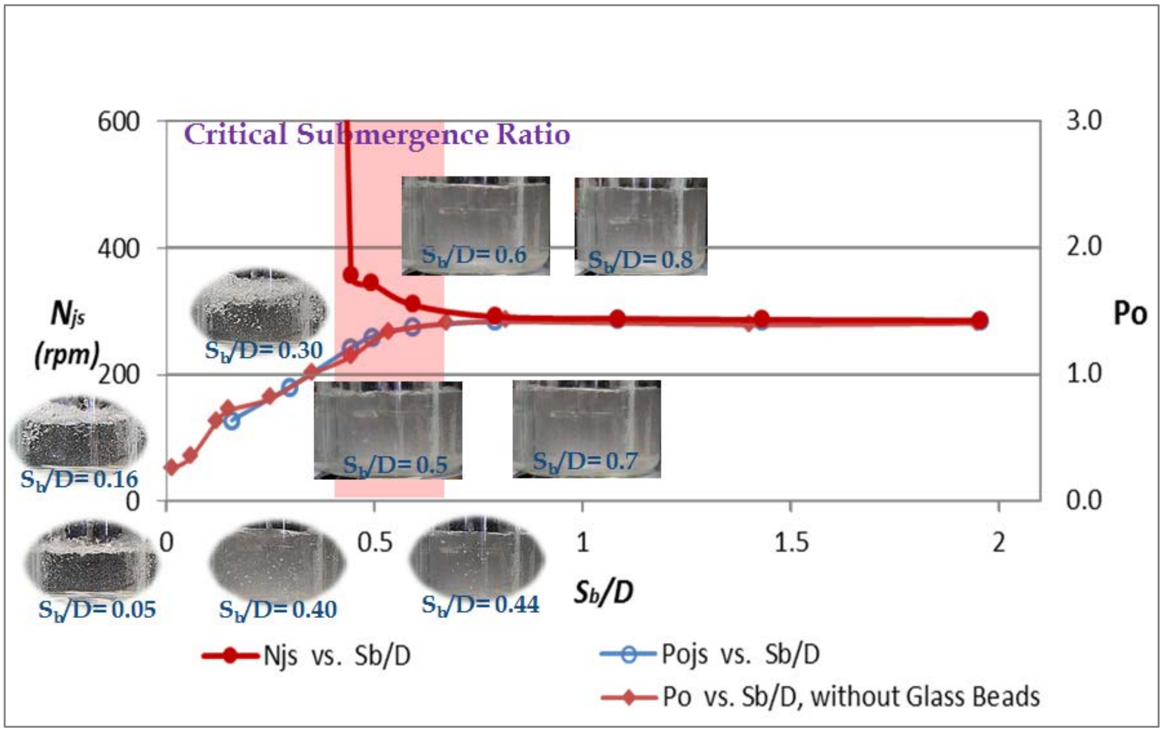

Figure 3.7 Minimum agitation speed and the relative power number for complete off-bottom solid suspension (N_{js}) as a function of impeller submergence ratio for C/T=1/3. (And the power number, Po, for different S_b/D in tank #3 with PBT3 without glass beads gotten in Section 3.1.)

CONCLUSION

In this work, the effect of the S_b/D ratio and the C_b/T ratio, as well as D/T ratio on the impeller Power Number for six-blade, 45^0 pitch-blade turbine impellers in flat bottom baffled tanks was studied.

When the impeller submergence ratio, S_b/D, is higher than a critical value $(S_b/D)_{cr}$, the impeller power number, *Po*, is constant and nearly independent on impeller submergence. However, below this critical submergence ratio, the impeller Power Number was found to decrease drastically. In this range, the impeller power number was almost directly proportional to S_b/D when for $S_b/D<(S_b/D)_{cr}$. For $H=T$, Po was nearly constant for different impeller off-bottom clearance ratios (C_b/T) from 0.2 to 0.8. Po is also affected by the *D/T*, but it is mainly affected by the S_b/D and the C_b/T.

For each tank system and *D/T*, there is a minimum value of the S_b/D to achieve complete off-bottom solids suspension. This value is the same value at which Po was shown become a function of S_b/D. For S_b/D higher than critical value, *Po* was constant and independent on S_b/D; however, when S_b/D was lower than the critical value, *Po* decreased and became almost directly proportional to the *Sb/D* ratio. The results obtained here for the minimum agitation for solid suspension, N_{js}, confirm that a stirred vessel operating at low impeller submergence is more likely to experience impeller flooding conditions where the impeller loses its ability to provide adequate liquid pumping, thus resulting in poor mixing performance.

APPENDIX

Data

The mainly data used in Chapter 3 are shown in below.

Table A.1 Power number, *Po*, for different S_b/D or S_b/T ratios in different combination of impellers and stirred baffled tanks at *C/T*=1/3

(a) Power Number for *D/T*=0.41, Tank #2, PBT3

S_b/D	S_b/T	Tank	Impeller	*N* (rpm)	*Po*	*Re*	*Fr*
1.68	0.69	Tank #2	PBT3	351	1.377	68799	0.463
1.22	0.50	Tank #2	PBT3	401	1.379	68796	0.463
0.71	0.29	Tank #2	PBT3	401	1.349	68831	0.463
0.53	0.22	Tank #2	PBT3	402	1.316	68875	0.464
0.43	0.18	Tank #2	PBT3	402	1.241	68695	0.461
0.34	0.14	Tank #2	PBT3	401	0.855	68572	0.460
0.24	0.10	Tank #2	PBT3	400	0.691	68584	0.460
0.14	0.06	Tank #2	PBT3	400	0.497	68674	0.461
0.04	0.02	Tank #2	PBT3	401	0.202	68694	0.461

(b) Power Number for *D/T*=0.35, Tank #3, PBT3

S_b/D	S_b/T	Tank	Impeller	*N* (rpm)	*Po*	*Re*	*Fr*
1.95	0.69	Tank #3	PBT3	423	1.398	40097	0.514
1.40	0.49	Tank #3	PBT3	351	1.386	33285	0.354
0.82	0.29	Tank #3	PBT3	401	1.411	38009	0.462
0.68	0.24	Tank #3	PBT3	401	1.396	37979	0.461
0.53	0.19	Tank #3	PBT3	402	1.325	38085	0.464
0.44	0.16	Tank #3	PBT3	400	1.133	37907	0.460
0.35	0.12	Tank #3	PBT3	401	0.995	38016	0.462
0.25	0.09	Tank #3	PBT3	401	0.802	37901	0.459
0.15	0.05	Tank #3	PBT3	401	0.708	38012	0.462
0.12	0.04	Tank #3	PBT3	400	0.612	37912	0.460
0.06	0.02	Tank #3	PBT3	400	0.341	37948	0.461
0.02	0.01	Tank #3	PBT3	400	0.248	37899	0.459

Table A.2 Power number for different C_b/T, H/T=1, D/T=0.26 or 0.35 (Tank #3, PBT2 and 3)

S_b/D	C_b/T	Impeller	N (rpm)	Po	Re	Fr
3.65	0.045	PBT2	487	1.877	46173	0.507
3.32	0.132	PBT2	491	1.764	46560	0.516
2.99	0.219	PBT2	494	1.685	46823	0.521
2.68	0.298	PBT2	494	1.637	46781	0.520
2.61	0.319	PBT2	488	1.592	46222	0.508
2.36	0.382	PBT2	496	1.541	47037	0.526
2.05	0.465	PBT2	495	1.520	46875	0.523
1.34	0.649	PBT2	496	1.545	46955	0.524
0.76	0.801	PBT2	496	1.493	46999	0.525
2.69	0.052	PBT3	492	1.748	84258	0.694
2.22	0.219	PBT3	492	1.487	84373	0.518
1.95	0.312	PBT3	450	1.416	77056	0.432
1.86	0.347	PBT3	450	1.402	77125	0.432
1.61	0.434	PBT3	450	1.431	77151	0.433
1.61	0.434	PBT3	452	1.433	77375	0.435
1.25	0.559	PBT3	451	1.519	77210	0.433
0.97	0.659	PBT3	451	1.500	77234	0.434
0.62	0.781	PBT3	451	1.463	77326	0.435

Table A.3 Minimum agitation speed (N_{js}), Minimum Power (P_{js}) and relative Power Number (*Po*) for Different Off-Bottom Clearance Ratio (C_b/T) at *D/T*=0.31 or *D/T*=0.41 and *H/T*=1. (Tank #2, PBT2 and PBT3)

C_b/T	S_b/D	N_{js} (rpm)	*P* (Watts)	*Po*	*Re*
D/T = 0.31, 0.5% *w/w* (Tank #2, PBT2)					
0.447	1.804	494	1.945	1.429	46815
0.407	1.936	461	1.633	1.480	43656
0.366	2.069	442	1.503	1.541	41898
0.325	2.202	404	1.216	1.636	38273
0.285	2.334	384	1.103	1.721	36426
0.244	2.467	356	0.950	1.864	33749
0.203	2.599	314	0.677	1.936	29760
0.163	2.732	297	0.596	2.026	28096
0.122	2.865	293	0.598	2.107	27770
0.081	2.997	288	0.588	2.183	27281
0.041	3.130	286	0.607	2.296	27113
D/T = 0.41, 0.5% *w/w* (Tank #2, PBT3)					
0.691	0.750	457	7.119	1.499	78376
0.650	0.848	444	6.673	1.531	76171
0.610	0.947	409	5.357	1.576	70114
0.528	1.144	399	5.037	1.601	68333
0.447	1.341	370	4.046	1.616	63325
0.407	1.440	302	1.974	1.451	51673
0.366	1.538	239	1.029	1.516	40978
0.285	1.736	223	0.883	1.594	38288
0.203	1.933	212	0.834	1.759	36363
0.122	2.130	223	1.029	1.874	38179
0.078	2.229	195	0.736	2.004	33400
0.041	2.327	169	0.520	2.164	28985

Table A.4 Minimum Agitation Number (N_{js}) and the Relative Power Number (Po_{js}) for Different Impeller Submergence Ratio(S_b/D) at different D/T and C_b/T ratios

S_b (cm)	H(cm)	H/T	S_b/D	N_{js} (rps)	N_{js} (rpm)	P(Watts)	Po
			D/T=0.40 (*Tank* #1, PBT2), C_b/T=0.3				
13.23	18.90	1.00	1.75	5.60	336	0.888	2.07
12.29	17.96	0.95	1.63	5.48	329	0.830	2.07
11.34	17.01	0.90	1.50	5.66	340	0.885	2.00
10.40	16.07	0.85	1.38	5.89	354	0.956	1.92
9.45	15.12	0.80	1.25	5.45	327	0.772	1.95
8.51	14.18	0.75	1.13	5.57	334	0.833	1.98
7.56	13.23	0.70	1.00	5.51	331	0.883	2.16
6.62	12.29	0.65	0.88	5.41	324	0.814	2.12
5.67	11.34	0.60	0.75	5.49	329	0.846	2.10
4.73	10.40	0.55	0.63	5.48	329	0.823	2.05
3.78	9.45	0.50	0.50	5.70	342	0.891	1.98
			D/T=0.31 (Tank #2, PBT2), C_b/T=0.3				
17.22	24.60	1.00	2.28	6.94	417	1.635	2.00
15.99	23.37	0.95	2.12	6.95	417	1.656	2.02
14.76	22.14	0.90	1.96	6.94	417	1.640	2.01
13.53	20.91	0.85	1.79	7.07	424	1.723	2.00
12.30	19.68	0.80	1.63	6.91	415	1.640	2.04
11.07	18.45	0.75	1.47	7.03	422	1.697	2.01
9.84	17.22	0.70	1.31	7.25	435	1.947	2.10
8.61	15.99	0.65	1.14	8.09	485	2.963	2.30
7.38	14.76	0.60	0.98	8.08	485	3.080	2.40
6.15	13.53	0.55	0.82	8.07	484	2.879	2.25
4.92	12.30	0.50	0.65	8.04	482	2.583	2.04
			D/T=0.35 (Tank #3, PBT3), C_b/T=0.31(C/T=1/3)				
19.82	28.82	1.00	1.95	4.76	286	1.658	1.43
14.50	23.50	0.82	1.43	4.78	287	1.680	1.43
11.00	20.00	0.69	1.08	4.81	289	1.722	1.44
8.00	17.00	0.59	0.79	4.87	292	1.757	1.42
6.00	15.00	0.52	0.59	5.18	311	2.047	1.38
5.00	14.00	0.49	0.49	5.74	344	2.637	1.30
4.50	13.50	0.47	0.44	5.94	357	2.733	1.22
			S_b/D below 0.44, glass beads cannot be suspended.				
3.00	12.00	0.42	0.30	5.88	353	1.971	0.90
1.60	10.60	0.37	0.16	5.88	353	1.400	0.64

REFERENCES

Armenante, P. M., Mazzarotta, B., & Chang, G. M. (1999). Power consumption in stirred tanks provided with multiple pitched-blade turbines. *Industrial & Engineering Chemistry Research*, 38(7), 2809-2816.

Armenante, P.M., Uehara-Nagamine, E. (1998). Determination of correlations to predict the minimum agitation speed for complete solid suspension in agitated vessels. *Canadian Journal of Chemical Engineering*, *76*, 413-419

Armenante, P. M., Uehara-Nagamine, E. (1998). Effect of low off-bottom impeller clearance on the minimum agitation speed for complete suspension of solids in stirred tanks. *Chemical Engineering Science*, *53(9),* 1757-1775

Chapple, D., Kresta, S. M., Wall, A., & Afacan, A. (2002). The effect of impeller and tank geometry on power number for a pitched blade turbine. *Chemical Engineering Research and Design*, 80(4), 364-372.

Motamedvaziri, S., Armenante, P.M. (2012). Flow regimes and surface air entrainment in partially filled stirred vessels for different fill ratios. *Chemical Engineering Science, 81*, 231-250.

Motamedvaziri, S. (2012). Single and Multiphase Mixing in Partially Filled Stirred Vessel. From http://archives.njit.edu/vol01/etd/2010s/2012/njit-etd2012-009/njit-etd2012-009.pdf.

Myers, K.J., Reeder, M.F., Fasano, J.B. (2002). Optimize Mixing by Using the Proper Baffles. *Chemical Engineering Progress*, *98.2*, 42-47

Sharma, R. N., Shaikh, A. A. (2003). Solids suspension in stirred tanks with pitched blade turbines. *Chemical Engineering Science, 58(10)*, 2123-2140.

Zhou, A. (2014). Experimental Determination of the Mixing Requirement for Solid Suspension in Pharmaceutical Stirred Tank Reactors. From http://archives.njit.edu/vol01/etd/2010s/2014/njit-etd2014-084/njit-etd2014-084.pdf

Zwietering, T. N. (1958). Suspending Solid Particles in Liquids by Agitators. *Chemical Engineering Science*, *8*, 244-253